Investigation of corrosion inhibition by Cassava leaf DNA on AISI 1015 low carbon steel in sodium chloride solution

I.E. Ekere,[1]* O. Agboola,[1] S.O.I. Fayomi,[2] A.O. Ayeni[1] and A. Ayodeji[1]

[1]Department of Chemical Engineering, Covenant University, Km. 10 Idiroko Road, Canaan Land, Ota, Ogun State, Nigeria
[2]Department of Mechanical and Biochemical Engineering, Bells University, Km. 8 Idiroko Road, Benja village 112104, Ota, Ogun State, Nigeria
**E-mail: isaacekere2@gmail.com*

Abstract

In the past few years many corrosion inhibitors research has been oriented towards eco-friendly extracts from plants. In this research cassava (*Manihot esculenta*) leaf Deoxyribonucleic acid (DNA) was extracted as green inhibitor compound for low carbon steel protection from corrosion. The mechanism of inhibition was investigated in 3.5% w/v NaCl (simulating naturally aerated seawater) by weight loss, potentiodynamic polarization measurements and SEM/EDX and FTIR assessments. These measurements investigated the corrosion resistance and morphology of low carbon steel using electrochemical parameters (corrosion potential, corrosion current and corrosion rate) and gravimetric analysis (weight loss and surface coverage). The electrochemical (potentiodynamic polarization) test results showed that a concentration of 20 mg/L of DNA, inhibited the corrosion of low carbon steel in 3.5% w/v NaCl with an inhibition efficiency of 96.4%. Inhibition efficiency of 88.37% from weight-loss measurements after immersion in the test solution for 240 hours were obtained as well. Potentiodynamic polarization tests plots demonstrated that DNA is a mixed inhibitor; it reduces both cathodic and anodic reactions by forming films on the surface of mild steel. The adsorption model of DNA corresponds to the Langmuir isotherm. This demonstrated the suitability of cassava leaf DNA as an inhibitor of mild steel corrosion for saline environment.

Received: February 26, 2022. Published: April 7, 2023 doi: 10.17675/2305-6894-2023-12-2-3

Keywords: *mild steel corrosion, NaCl solution, plant DNA, potentiodynamic polarization, adsorption.*

1. Introduction

Studies have shown that there is a significant durability problem associated with the corrosion of steel in 3.5 wt. percentage solution of NaCl [1, 2], steel-reinforced concrete structures exposed to chloride ions [3, 4] and CO_2 saturated NaCl solution [5, 6]. Among well-known aggressive media and agents, chloride ions constitute a major steel-bar corrosion inducing agents. These chloride ions are usually found in artificial saline environment are brought into contact with when de-icing salts is used in temperate regions. Chloride ions do

not form hard soluble salts with iron ions, unlike other metals; therefore, the presence of chlorides in an environment will cause steel to corrode.

The application of inhibitors is one of the most common ways to reduce corrosion and protect metals. The use of synthetic inhibitors, though efficient, has come under intense scrutiny due to environmental regulations. Plant extracts and animal products, organic in nature, low-cost, biodegradable and less deleterious, have been well documented to demonstrate anti-corrosive activity on mild steel corrosion [7–11]. This work reports an investigation into the activity of plant (cassava) leave DNA as an eco-friendly corrosion inhibitor.

In 2017, Hu *et al.* [12] presented the first reported investigation of biomacromolecular DNA as green inhibitor to protect x80 steel. The studies utilized DNA from Salmon fish, which demonstrated an inhibition efficiency of 91%. The results were obtained after gravimetric tests and potentiodynamic polarization, followed by quantum chemical calculation and FITR. The adsorption followed the Langmuir adsorption model. Jiang *et al*. (2017) [2] proposed new findings using a mixed solution of olignonucleotide, ranging in length from 20–80 nucleotides DNA as an inhibitor. This olignonucleotide, used in a simulated concrete pore solution, performed well as biological corrosion inhibitor of steel reinforcement in a chloride-containing solution. Also, Agboola *et al*. (2019) [13], following in the same vein reported the adsorptive performance of the calf thymus gland DNA (CTG_{DNA}) as a corrosion inhibitor in acidic medium on 3CR12 stainless steel, this with very promising and eco-friendly results. These studies clearly show a promising start for biomacromolecular DNA in corrosion research. DNA adsorbs unto the metal surface and forms films that does not wear-off with flow [3]. Only a handful of research works have investigated the use of DNA as a corrosion inhibitor [13]. In literature, DNA application as a corrosion inhibitor is still in its early stage of development. Spurred by the knowledge that plant DNA is readily available as the major ingredient needed is a cell [3, 14, 17] we have ventured into the use, for the first time been reported, of plant leaf DNA solution as a corrosion inhibitor. This research has as its main objective the evaluation of the corrosion inhibitor performance of cassava leaf DNA for mild steel in 3.5% w/v NaCl. This performance was assessed by determining the inhibition efficiency through potentiodynamic polarization and weight loss and surface examination.

2. Experimental Methods

2.1. Mild steel sample preparation

Small mild steel sample coupons of length 2.4 cm by width 1.55 cm by thickness 0.15 cm each were cut into rectangular shapes. A small hole was bored into each coupon from which the sample was suspended. SiC abrasive paper of standard ANSI 400, 600 and 800 grit were then used to mechanically polish the coupons. After this, the surfaces of the coupons were degreased with ethanol and acetone. Distilled water was then applied to rinse the surface and dried with heat from a hot plate, while being held over it. Mild steel is a type of carbon steel

with low amount of carbon alloyed with iron ranging from 0.05–0.25% carbon, by weight. There is also a small concentration of other elements in the alloy such as chromium, aluminum, manganese and nickel. This is shown in Table 1 as obtained from analysis.

Table 1. AISI 1015 mild steel elemental composition.

Element	Fe	C	Mn	Si	Al	Cr	P	S	Ni
%Composition	99.2	0.15	0.43	0.17	0.006	0.001	0.02	0.033	0.007

2.2. Preparation of corrosive media, 3.5% w/v NaCl

Ocean seawater, constituting the archetypal source of mineralization and corrosion phenomena, is approximately 3.5% w/v of sodium chloride, NaCl, [15, 16]. The sodium chloride media, which simulates seawater, made by dissolving 3.5 g of NaCl crystal in 100 ml of distilled water, contained the typical concentration of chloride ion in natural seawater.

2.3. Extraction of cassava leave DNA

The first step in extraction is to choose the plant part that contains the major concentration of the active compound of interest. In this study, the DNA from cassava was extracted from the leaves because isolating DNA from leaves is easy. Leaves were also chosen because they exist in larger amounts than other plant tissues, possess greater cell wall to area ratio, so made the extraction of larger proportion of DNA possible. In addition, young, freshly cut leaves were chosen because they have less phenolic compounds and are not lignified (free of secondary metabolites, which increased the ease cell walls disruption). The young and tender cassava leaves were finely cut with a kitchen knife after they were washed with distilled water and then leaf midrib and petioles removed before blending. Petioles and leaf midrib bring about carbohydrate contamination during extraction. 150 g of the finely cut cassava leaves were crushed in a mortar, bringing about the disruption of plant cell wall. 100 ml of centrimoium bromide (CTAB) extraction buffer is poured into the vessel with crushed leaves and then placed in an incubator at 65°C and left for 2 days. The tubes containing the mixture was inverted from time to time during the incubation. The mixture was then decanted and 50 ml of isoamyl alcohol and chloroform (1:24 ratio) was added. This mixture was spun in the centrifuge at 2300 rpm for 2 minutes at room temperature. 6 ml of ammonium acetate was added to the supernatant (topmost aqueous layer) obtained after centrifugation and gently stirred until the appearance of DNA. This mixture was spun again for 5 minutes at 2300 rpm in the centrifuge and the supernatant above the formed pellet of DNA discarded leaving the strands of DNA. To obtain DNA of higher purity it is washed with absolute ethanol. 8 ml of ethanol was pipetted into the tube with DNA strands and centrifuged at a speed of 2300 rpm for an interval of 5 minutes. The supernatant was poured out afterwards and the DNA strands retained. [14, 17, 18]. DNA concentration and purity was ascertained by the measurement of absorbance in a Thermo Scientific NanoDrop 2000

UV Visible spectrophotometer using the principle of light absorbance. DNA purity for practical purposes will have an absorbance ratio, A260/A280, range from 1.7–2.0 [14]. An absorbance ratio of 1.6 is acceptable for corrosion inhibition application. A DNA concentration less than 1.6 is an indication of a contamination. This is will affect the results of the corrosion experiment.

3. Experimental procedure

3.1. Gravimetric (weight-loss) measurements

The cleaned and polished mild steel coupons are submerged in a 250 ml beaker containing salt solutions, with and without 5–20 mg/l cassava leave DNA for 240 hours (10 days) at room temperature. Afterwards the steel samples were taking out of the test solution, cleaned with brush and bathed in copious quantity of distilled water, dried out and then weighed. The weight loss measures were used to calculate the corrosion rate according to Equation (1):

$$\text{Corrosion rate } C_{\mathrm{R}} = \frac{m_1 - m_2}{At} \tag{1}$$

m_1, m_2 – weights (in grams) of the metal coupons in the absence and presence of the inhibitor. A represents the mild steel coupon surface area (in cm^2) and t, time (hours) [19].

The inhibition efficiency (η) and surface coverage (Θ) were obtained using the following equations:

$$\eta\% = \frac{C_{\mathrm{R}} - C_{\mathrm{R(i)}}}{C_{\mathrm{R}}} \cdot 100 \tag{2}$$

$$\Theta = \frac{C_{\mathrm{R}} - C_{\mathrm{R(i)}}}{C_{\mathrm{R}}} \tag{3}$$

where C_{R} and $C_{\mathrm{R(i)}}$ are the corrosion rates in the uninhibited and inhibited solution, respectively.

3.2. Electrochemical measurements

An Autolab Nova 2.1.1 Potentiostat model 273A interfaced with a personal computer software for linear polarization studies investigated corrosion by electrochemical means. Polarization tests evaluate current produced by variable voltage in the working electrode. It employed a conventional three-electrode electrochemical cell. Mild steel samples with 3.72 cm^2 exposed geometrical square surface area were embedded in polytetrafluoroethylene (PTFE) after cleaning as described above. The mild steel functioned as the working electrode, platinum electrode as the counter/auxiliary electrode, and a saturated calomel electrode (SCE) served as the reference electrode. The SCE (0.241 V/SHE) is the reference potential used in this work. The potentiodynamic polarization tests were conducted in naturally aerated and unstirred solutions of 3.5% w/v NaCl with and without 5, 10, 15 and

20 mg/l DNA of cassava leave at room temperature. The corrosion parameters were then logged after the open circuit potential of the working electrode was established and applying a potential range from ±250 mV OCP with a scan rate of 0.3 mV/s. To ensure that each corrosion parameter was reproduced, each test was run in 3 times [19].

3.3. Surface characterization

Surface characterizations are conducted by means of microscopy (*e.g.* SEM) and spectroscopic (*e.g.* XPS) methods. Scanning electron microscopes, (SEM) was used for the morphological examination of the surfaces of the AISI 1015 mild steel samples. This characterization provided a clear comparison between the metal surfaces with and without the DNA inhibitor.

4. Results and Discussion

4.1. Gravimetric (weight-loss) analysis

The inhibition efficiency of cassava leave DNA was examined by obtaining the loss in weight of the metal samples after exposure to the salt solution in the absence and presence of DNA of different concentrations in the corrosive medium, unstirred 3.5% w/v NaCl solution, a simulation of natural seawater, at ambient temperature. The corrosion parameters for weight loss obtained from these measurements are summarized in Table 2 and Figure 1.

Table 2. Weight loss information for mild steel immersed in 0–20 mg/l of cassava leave DNA in 3.5%w/v NaCl at room temperature.

Cassava DNA Conc. (mg/l)	Weight of sample before immersion (g)	Weight of sample after immersion (g)	Loss in mass (g)	Surface area (cm^2)	Corrosion rates (mg/cm^2 hr)	Efficiency of inhibition η%	Surface coverage Θ
Blank	4.1804	4.1082	0.0722	7.5	$4.011 \cdot 10^{-5}$	0.00	0
5	4.459	4.4411	0.0179	7.5	$9.944 \cdot 10^{-6}$	75.21	0.7521
10	4.8352	4.8251	0.0101	7.5	$5.611 \cdot 10^{-6}$	86.01	0.8601
15	4.6087	4.5993	0.0094	7.5	$5.222 \cdot 10^{-6}$	86.98	0.8698
20	4.5918	4.5834	0.0084	7.5	$4.666 \cdot 10^{-6}$	88.37	0.8837

Table 2 shows weight loss calculation, corrosion rate and inhibitor efficiency for different concentrations. Without DNA, inhibitor corrosion rate is 0.04 $\mu g/cm^{-2} h^{-1}$. Corrosion rate reduces to 0.00994 $\mu g/cm^{-2} h^{-1}$ upon introduction of 5 mg/L inhibitor and then to as low as 0.0047 $\mu g/cm^{-2} h^{-1}$ with a highest inhibition efficiency of 88.4% at 20 mg/L concentration. This indicate that corrosion rate decreased as a function of the increasing plant DNA concentration. The increase in the inhibition efficiency also corresponds to the increase in DNA inhibitor concentration.

4.2. Electrochemical measurements (potentiodynamic polarization)

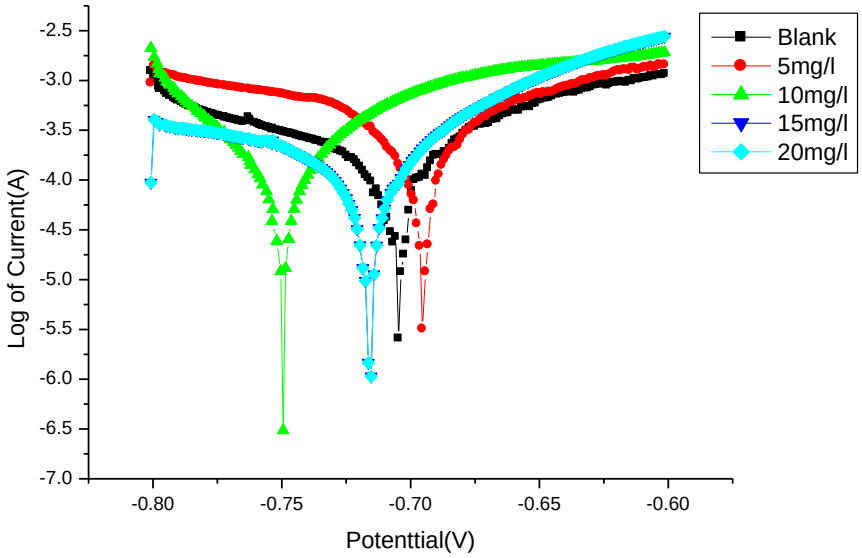

Figure 1. Anodic and cathodic polarization curves of mild steel in 3.5% w/v NaCl solution with 0–20 mg/l concentrations of cassava DNA at 298 K.

It can be seen from Figure 1, anodic and cathodic polarization curves for mild steel in 3.5% w/v NaCl solution with 0–20 mg/l cassava DNA as inhibitor, that the corrosion potential, E_{corr} of the uninhibited steel, represented by the black curve is –705 mV, an indication of active metal dissolution. This value is as expected for corrosion reactions in saline solutions. DNA inhibitor addition shifts the polarization plots cathodically, the corrosion potential becomes more negative and current densities lower in all concentrations (except for 5 mg/l) than in the blank with the –750 mV as the maximum. This shift of potential towards the left of the graph, the cathodic region, a change from active to passive potential range, an indication of the reduction of oxygen reaction rate, demonstrates the good quality of the film formed by the inhibitor to protect the mild steel. The mechanism of inhibition of cassava leaf DNA is obtained by comparing the polarization curves of the blank and inhibited solutions. Corrosion potential shifts to the cathodic region, especially for the 10, 15 and 20 mg/l concentrations. From Figure 1, we see that inhibitors rarely affect the anodic and cathodic reactions equally. The diagram illustrates the classification of anodic and cathodic inhibitors: in lowering the i_{corr}, E_{corr} shifts negatively indicating cathodic inhibitor. While E_{corr} may give a preliminary indication of the inhibition mechanism, polarization curves gives a more complete assessment. The displacement in potential value with and without DNA inhibitor addition from –705 mV to –690 mV is 15 mV, less than 85 mV. This result show DNA to be a cathodic type inhibitor [12].

4.3. SEM/EDX surface analysis

The surface morphology of the steel microstructures was analyzed by SEM-EDX. Mild steel surface exposed to the corrosive media, 3.5% w/v NaCl, was severely corroded and very

rough and non-uniform. Figure 2(a) shows the significant corrosion damage done to the steel surface. The EDX elemental composition confirmed the SEM pictures with large amounts of iron and oxygen values of 64.6% and 28.36% due to the formation of corrosion products, oxides and chlorides of iron, covering the surface of the steel (Figure 2(b)(c)). The surface morphologies of steel immersed in inhibitor are significantly improved and shows a smoother surface with scratches left behind after grinding, but without corrosion damage (Figure 3(a)). The EDX analysis for the inhibited system shows (Figure 3(b, c)) oxygen in smaller percentage, 10.84%, which can be related to chemisorption (adsorption) of plant DNA on the mild steel surface. The DNA displaces the oxygen and water molecules leading to a limited iron oxides formation.

(a)

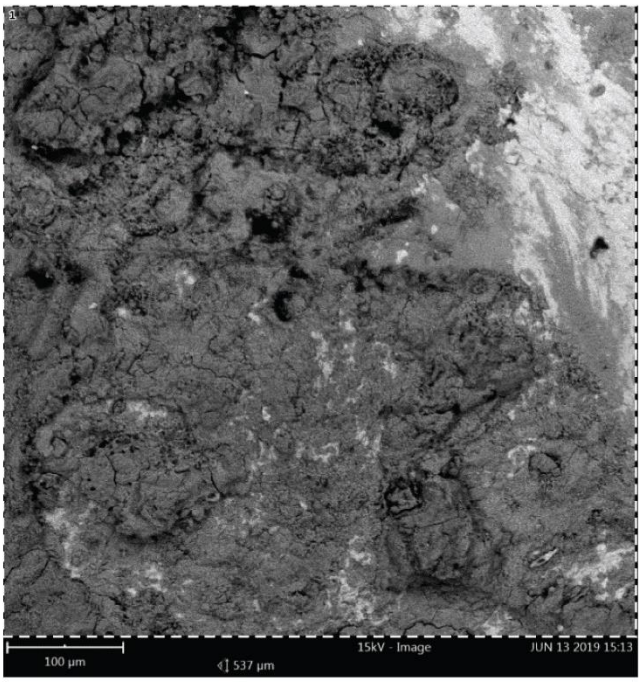

(b)

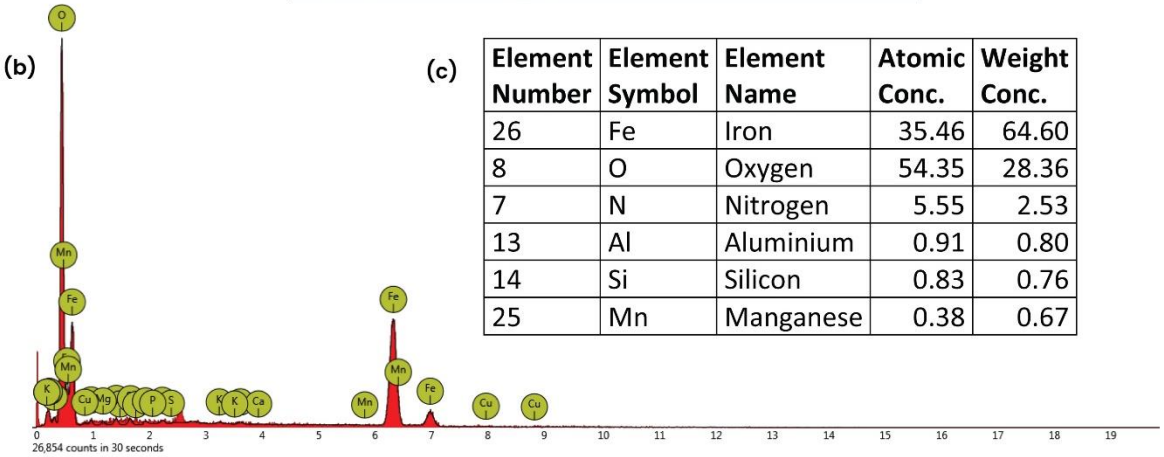

(c)

Element Number	Element Symbol	Element Name	Atomic Conc.	Weight Conc.
26	Fe	Iron	35.46	64.60
8	O	Oxygen	54.35	28.36
7	N	Nitrogen	5.55	2.53
13	Al	Aluminium	0.91	0.80
14	Si	Silicon	0.83	0.76
25	Mn	Manganese	0.38	0.67

Figure 2. (a) SEM Mild steel micrograph after immersion in NaCl solution in the presence; (b) Mild steel composition after immersion in NaCl solution with without DNA inhibitor; (c) Mild steel EDX spectra without DNA inhibitor in NaCl solution.

(a)

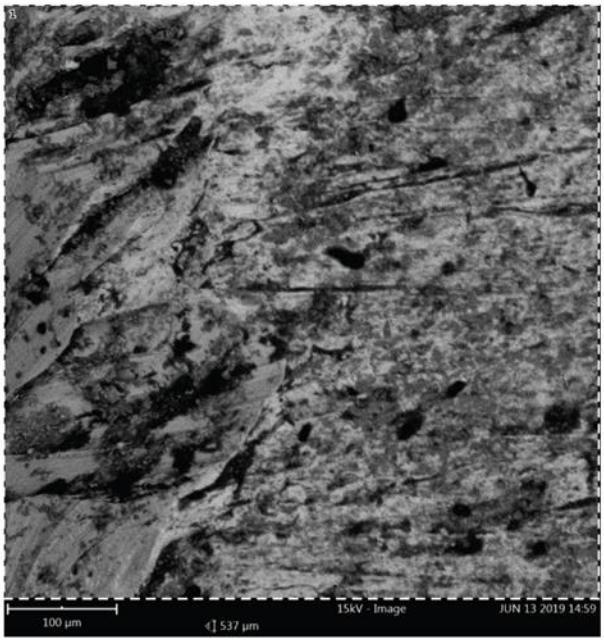

(b)

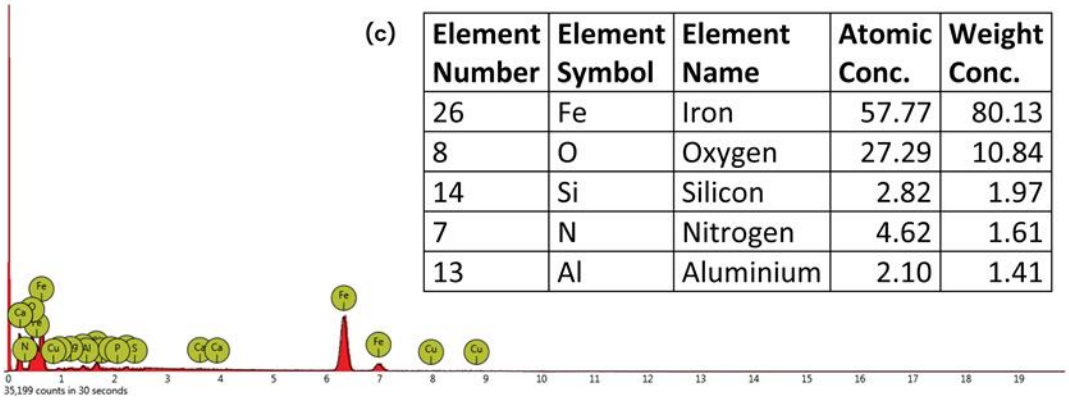

(c)

Element Number	Element Symbol	Element Name	Atomic Conc.	Weight Conc.
26	Fe	Iron	57.77	80.13
8	O	Oxygen	27.29	10.84
14	Si	Silicon	2.82	1.97
7	N	Nitrogen	4.62	1.61
13	Al	Aluminium	2.10	1.41

Figure 3. (a) SEM Mild steel micrograph after immersion in NaCl solution in the presence of 20 mg/l DNA inhibitor; (b) Mild steel composition after immersion in NaCl solution with 15 mg/l of DNA inhibitor; (c) Mild steel EDX spectra with 15 mg/l DNA inhibitor in NaCl solution.

4.3. FTIR spectral characterizations

FTIR analysis shows the properties of the adsorbed DNA layer. Figure 4, 5 and 6 show the FTIR spectra for pure cassava DNA inhibitor, mild steel surface after exposure in 3.5% solution of NaCl with 15 mg/L cassava DNA and without any inhibitor. The characteristics peaks representing functional groups frequencies for the FTIR spectra appear at the bottom. The presence of corrosion products, iron oxide and oxyhydroxide, on the steel surface is indicated by the peaks 1188.19 cm^{-1} (Figure 4). This happens with the exposure of the mild steel in the salt solution in the absence of DNA inhibitor. This characteristic peak for iron oxides disappears in the spectral for the reaction when 15 mg/l of the DNA inhibitor is introduced (Figure 5). The peaks 3348 cm^{-1} and 3309 cm^{-1} appearing in figure attributed to

surface bound water no longer appears in the Figure with introduction of 15 mg/l of the DNA inhibitor. The frequency of the functional group C=O (double bond stretching vibration), shown by a dip of 1643.39 cm^{-1} on the pure Cassava DNA FTIR spectral in Figure 4 is not seen in the mild steel spectral in Figure 6 showing that the absence of the DNA structure in the blank corrosion experiments. Table 3 gives a table that summarizes important peaks on the FTIR for the conditions with and without inhibitor and the correspondent attribution.

Table 3. Summary of important peaks on the FTIR for the conditions with and without inhibitor and the correspondent attribution.

Condition	Peaks	Correspondent attribution	Citation
Conditions with inhibitor	Guanine carbonyl vibrations occur at 1712.85, while cytosine occur at 1512.24 (Figure 5). Figure 6 shows pure DNA at 1643.39 cm^{-1}.	This peak is attributed to aromatic C=C bending which is also correlated to the G–C and A–T base pairs (DNA in-plane vibrations at 1750–1500 cm^{-1}).	[24], [25], [12]
Conditions without inhibitor	The presence of several peaks without uniformity and little or no adsorption tells that the functional groups present.		

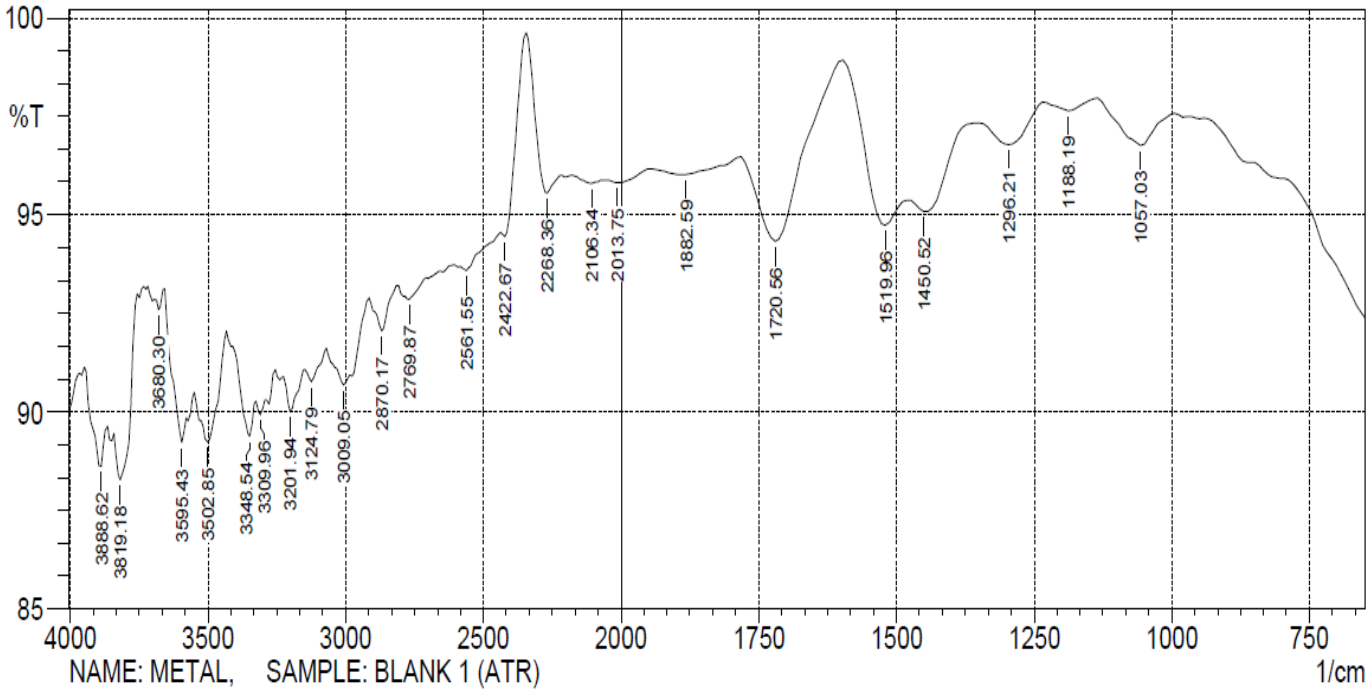

Figure 4. FTIR spectral of metal surface after exposure to NaCl solution in the absence of DNA inhibitor.

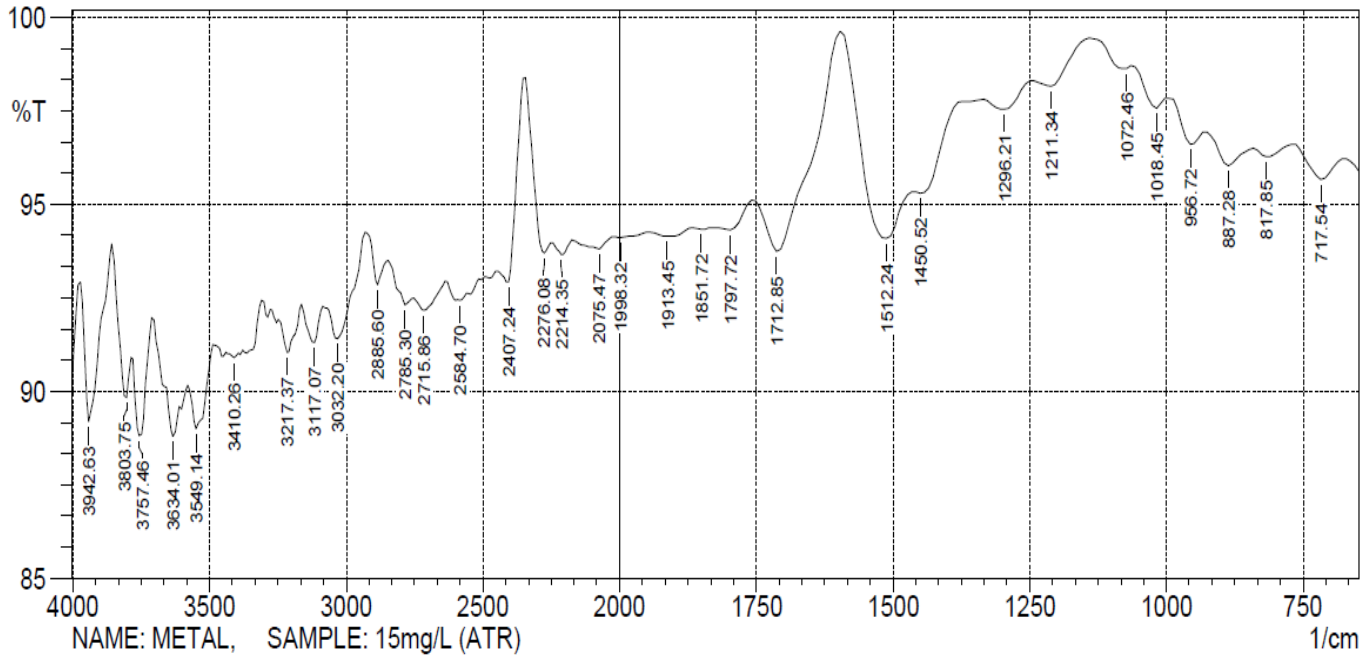

Figure 5. Mild steel FTIR spectral showing the characteristics frequencies of functional groups in DNA investigating corrosion inhibition with 15 mg/L cassava DNA inhibitor in solution of 3.5% NaCl.

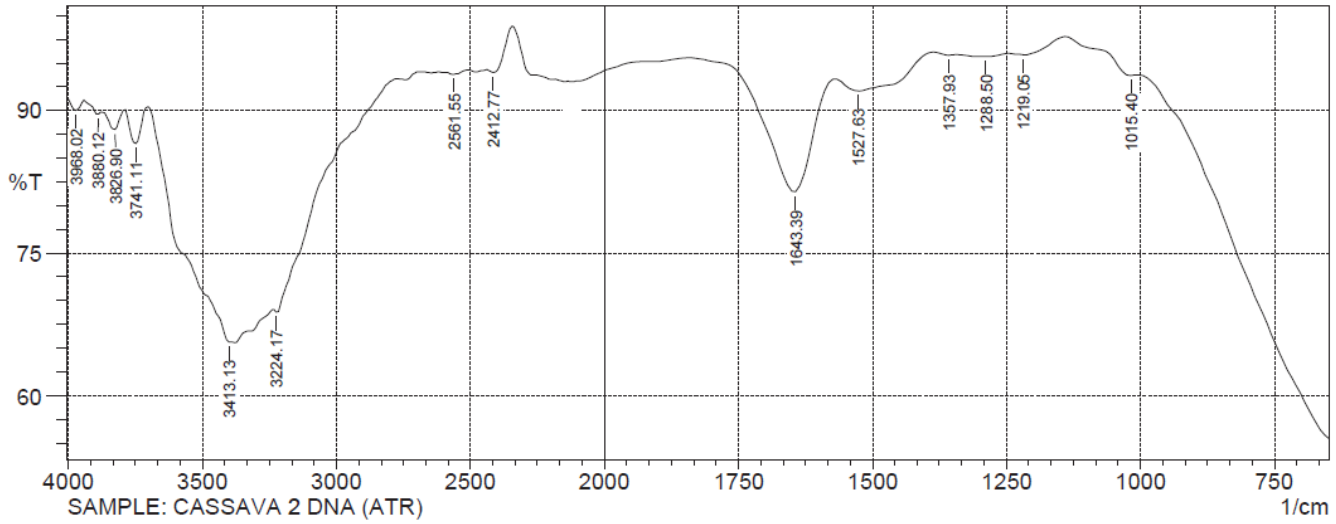

Figure 6. FTIR spectral showing the characteristics frequencies of functional groups in DNA for pure cassava DNA inhibitor.

4.4. Adsorption isotherms

Corrosion inhibition occurs because of adsorption of the molecules of the inhibitor on the metal surface, resulting in less reactive coverage. Data from weight loss measurements were fitted with different adsorption isotherm models in order to understand metal surface-inhibitor molecule interaction. The adsorption models include Langmuir, Temkin, Flory–

Huggins and Frumkin. The Langmuir isotherm, which can be seen in Figure 7, with a linear regression coefficient (R^2) of 0.9968, is indicative of monolayer adsorption of inhibitor molecule forming a protective film on the metal surface [22, 23].

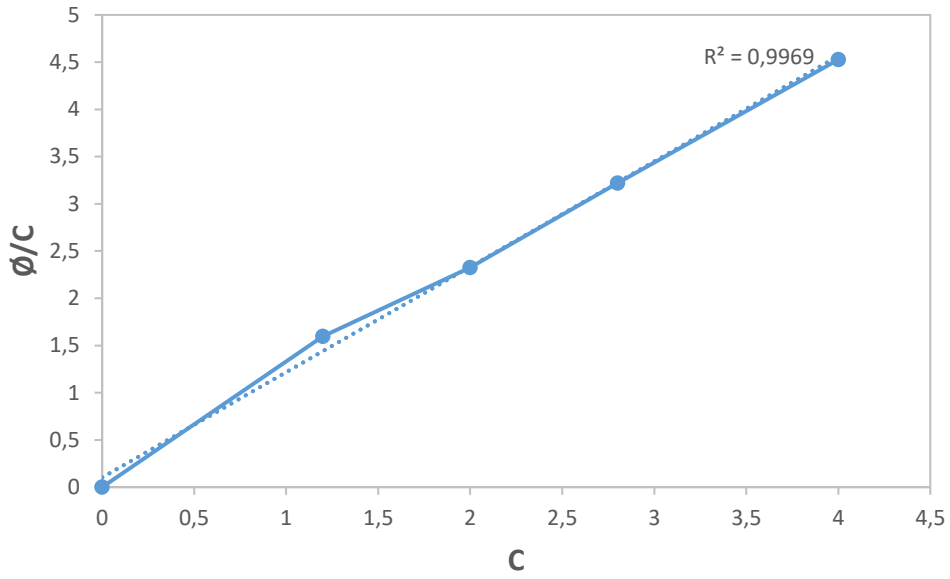

Figure 7. Langmuir adsorption isotherm for mild steel in 3.5% w/v NaCl with different concentrations of cassava DNA.

5. Conclusions

This study concludes as follows: Cassava leaf DNA worked as a highly effective standalone inhibitor for mild steel corrosion in 3.5% w/v NaCl. The laboratory mass loss test yielded an inhibition efficiency of 88.4% while the electrochemical techniques of potentiodynamic polarization yielded an inhibition efficiency of 96.4% for 20 mg/l concentration. It is worthy of note that small amounts of the DNA inhibitor in milligrams per liter resulted in greatly reduced mild steel corrosion rates in the salt solution. From plots obtained from potentiodynamic polarization, this study draws the conclusion that cassava leave DNA suppresses both anodic and cathodic reactions in the salt solution and hence is as a cathodic type inhibitor. Adsorption isotherm of cassava leave DNA in 3.5% w/v NaCl on mild steel follows the Langmuir adsorption isotherm.

SEM micrographs and EDX spectral analysis showed the smoothest surfaces and lowest oxygen levels respectively with 15 mg/L cassava DNA addition when mild steel was exposed to the corrosive environment, solution of 3.5% w/v NaCl. This is an indication of corrosion inhibition, showing a limited formation of iron oxide. FTIR micrographs indicating the appearance of DNA functional groups frequencies on the mild steel also reveal the adsorption of the plant DNA on the mild steel after the corrosion experiment.

Acknowledgement

The authors hereby appreciate Covenant University for sponsoring the publication of this article.

Conflict of interest

The corresponding author, on behalf of all authors hereby states that there is no conflict of interest.

References

1. S.J. Choi, H.S. Lee, J.W. Jang and S. Yi, Corrosion behavior in a 3.5 wt% NaCl solution of amorphous coatings prepared through plasma-spray and cold-spray coating processes, *Met. Mater. Int.*, 2014, **20**, 1053–1057. doi: 10.1007/s12540-014-6008-4
2. N. Kumar, M. Fusco, M. Komarasamy, R.S. Mishra, M. Bourham and K.L. Murty, Understanding effect of 3.5 wt.% NaCl on the corrosion of Al0.1CoCrFeNi high-entropy alloy, *J. Nucl. Mater.*, 2017, **495**, 154–163. doi: 10.1016/j.jnucmat.2017.08.015
3. S.B. Jang., L.H. Jiang, Z.Y. Wang, M. Jin, S. Bai, S. Song and X. Yan, Deoxyribonucleic acid as an inhibitor for chloride-induced corrosion of reinforcing steel in simulated concrete pore solutions, *Constr. Build. Mater.*, 2017, **150**, 238–247. doi: 10.1016/j.conbuildmat.2017.05.157
4. B. Pradhan, Corrosion behavior of steel reinforcement in concrete exposed to composite chloride–sulfate environment, *Constr. Build. Mater.*, 2014, **72**, 398–410. doi: 10.1016/j.conbuildmat.2014.09.026
5. J. Owen, C. Ramsey, R. Barker and A. Neville, Erosion-corrosion interactions of X65 carbon steel in aqueous CO_2 environments, *Wear*, 2018, **414–415**, 376–389. doi: 10.1016/j.wear.2018.09.004
6. A.S. Abbasov, A.A. Mamedxanova, H.M. Abd El-Lateef, L.I. Aliyeva, T.A. Ismayilov, C.I. Musayev, O.A. Aydamirov and F.A. Amirov, Prediction and measurements of corrosion inhibition of mild steel c1018 using some natural naphthenate surfactants in Co_2-saturted NaCl solution, *Res. J. Appl. Sci.*, 2014, **9**, no. 2, 66–75. doi: 10.3923/rjasci.2014.66.75
7. C.A. Loto, The effect of bitter leaf extract on the inhibition of mild steel in HCl and H_2SO_4, *Corros. Prev. Control*, 2003, **50**, no. 1, 43–49.
8. O.K. Aboila and A.O. James, The effects of *Aloe vera* extract on corrosion and kinetics of corrosion process of zinc in HCl solution, *Corros. Sci.*, 2010, **52**, no. 2, 661–664. doi: 10.1016/j.corsci.2009.10.026
9. P.C. Okafor and E.E. Ebenso, inhibitive action of carica papaya extracts on the corrosion of mild steel in acidic media and their adsorption characteristics, *Pigm. Resin Technol.*, 2007, **36**, 134–140. doi: 10.1108/03699420710748992
10. O. Olawale, J. Bello and P. Akinbami, *Int. J. Modern Eng. Res.*, 2015, **5**, 25–29.

11. E. Alibakhshi, M. Ramezanzadeh, G. Bahlakeh, B. Ramezanzadeh, M. Mahdavian and M. Motamedi, *Glycyrrhiza glabra* leaves extract as a green corrosion inhibitor for mild steel in 1 M hydrochloric acid solution: Experimental, molecular dynamics, Monte Carlo and quantum mechanics study, *J. Mol. Liq*., 2018, **255**, 185–198. doi: 10.1016/j.molliq.2018.01.144
12. K. Hu, J. Zhuang, J. Ding, Z. Ma, F. Wang and F. Zeng, Influence of biomacromolecule DNA corrosion inhibitor on carbon steel, *Corros. Sci*., 2017, **125**, 68–76. doi: 10.1016/j.corsci.2017.06.004
13. O. Agboola, F. Achile, S.O. Fayomi, S.E. Sanni, O. Abatan, E.R. Sadiku, P. Popoola, M.P. Mubiayi, E.T. Akinlabi, M.E. Makhatha, T. Adedoyin and I. Ekere, Adsorptive Performance Mechanism of the DNA of Calf Thymus Gland (CTG_{DNA}) on $3CR_{12}$ Stainless Steel as Corrosion Inhibitor in Acidic Medium, *J. Bio and Tribo corrosion*, 2019, **5**, 52. doi:10.1007/s40735-019-0245-5
14. J. Amani, R. Kazemi, A.R. Abbasi and A.H. Samanian, A simple and rapid leaf genomic DNA extraction method for polymerase chain reaction analysis, *Iran. J. Biotechnol*., 2011, **9**, no. 1, 69–71.
15. P.D. Williams, E. Guilyardi, G. Madec, S. Gualdi and E. Scoccimarro, The role of mean ocean salinity in climate, *Dynamics of atmosphere and oceans*, 2010, **49**, no. 2–3, 108–123. doi: 10.1016/j.dynatmoce.2009.02.001
16. K. Zakowiski, M. Narozny, M. Szocinski and K. Darowicki, Influence of water salinity on corrosion risk—the case of the southern Baltic Sea coast, *Environ. Monit. Assess*., 2014, **186**, no. 8, 4871–4879. doi: 10.1007/s10661-014-3744-3
17. K.C. Sika, T. Kefela, H. Adoukonou-Sagbsdja, L. Ahoton, A. Saidou, L. Baba-Mousa, L.J. Baptiste, S.O. Kotconi and E.W. Gachomo, A simple and efficient genomic DNA extraction protocol for large scale genetic analyses of plant biological systems, *Plant gene*, 2015, **1**, 43–45. doi: 10.1016/j.plgene.2015.03.001
18. J.J. Doyle and J.L. Doyle, A Rapid DNA Isolation Procedure for Small Quantities of Fresh Leaf Tissue, *Phytochem. Bull*., 1987, **19**, no. 1, 11–15.
19. A.S. Umoren, M.J. Banera, T. Alonso-Garcia, C.A. Gervasi and M.V. Mirifico, Inhibition of mild steel corrosion in HCl solution using chitosan, *Cellulose*, 2013, **20**, 2529–2545. doi: 10.1007/s10570-013-0021-5
20. E. Stupnisek-Lisac, A. Gazivoda and M. Madzarc, Evaluation of non-toxic corrosion inhibitors for copper in sulphuric acid, *Electrochim. Acta*, 2002, **47**, no. 26, 4189–4194.
21. F. Mansfield, *Corrosion*, 1973, **29**, 397–402.
22. A.O. Dada, A.P. Olalekan, A.M. Olatunya and O. Dada, Langmuir, Freundlich, Temkin and Dubinin-Radushkevich Isotherms Studies of Equilibrium Sorption of Zn^{2+} onto Phosphoric Acid Modified Rice Husk, *IOSR J. Appl. Chem*., 2012, **3**, no. 1, 38–45.
23. B.B. Damaskin, O.A. Petrii and V.V. Batrakov, *Adsorption of Organic Compounds on Electrodes*, New York-London: Plenum Press, 1971.

24. H.A. Tajmir-Riahi, C.N. N'soukepoe-Kossi and D. Joly, Structural analysis of protein–DNA and protein–RNA interactions by FTIR, UV-visible and CD spectroscopic methods, *J. Spectrosc*., 2009, **23**, 81–101. doi: 10.3233/SPE-2009-0371
25. J.A. Taboury, J. Liquier and E. Taillander, Characterization of DNA structures by infrared spectroscopy: double helical forms of poly(dG-dC)·poly(dG-dC), poly(dD^{8}G-dC)·poly(dD^{8}G-dC), and poly(dG-dm^{5}C)·poly(dG-dm^{5}C), *Can. J. Chem*., 1985, **63**, no. 7, 1904. doi: 10.1139/v85-315

♦ ♦ ♦